# In-flight characteristics of the space count of NOAA AVHRR channels 1 and 2

R.M. Mitchell

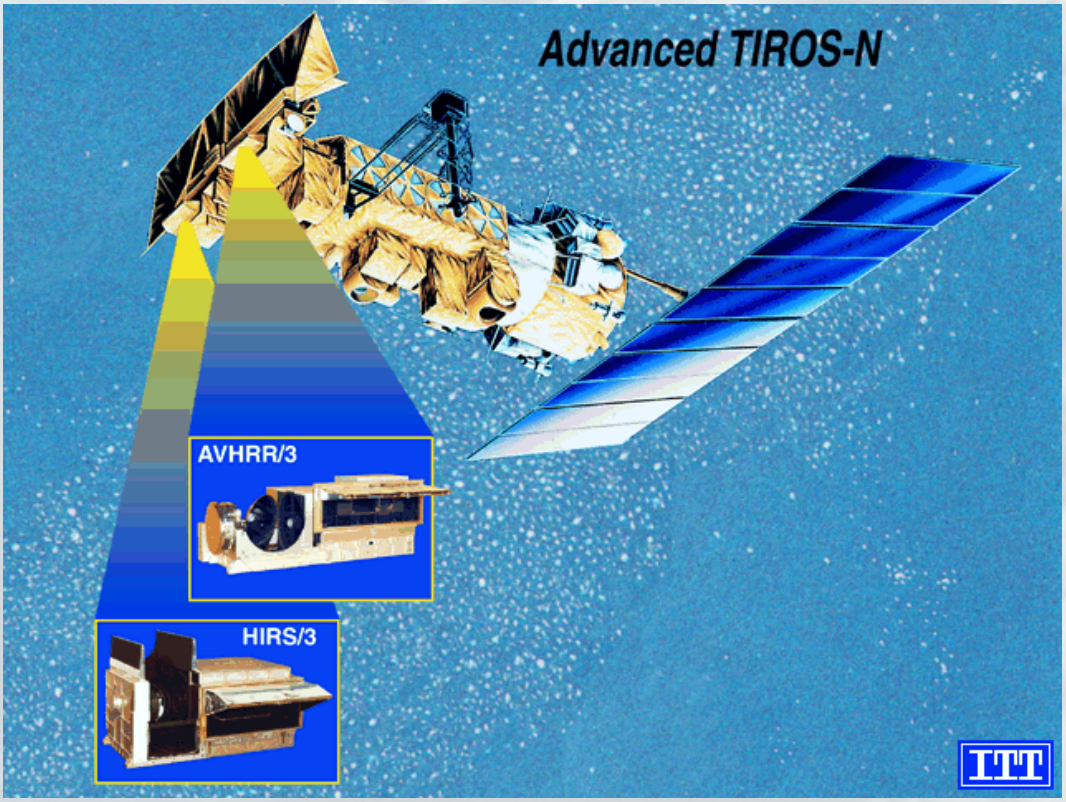


CSIRO

Atmospheric Research

CSIRO Atmospheric Research Technical Paper no. 52

# In-flight characteristics of the space count of NOAA AVHRR channels 1 and 2

**R.M. Mitchell**

CSIRO Atmospheric Research Technical Paper no. 52

**National Library of Australia Cataloguing-in-Publication Entry**

Mitchell, R.M. (Ross McGregor), 1954– .
In-flight characteristics of the space count
of NOAA AVHRR channels 1 and 2

Bibliography.
ISBN 0 643 06646 2

1. Scientific satellites. 2. Radiometers. 3. Meteorological instruments.
I. CSIRO. Division of Atmospheric Research.
II. Title. (Series: CSIRO Atmospheric Research technical paper; no. 52).

551.6354

Address and contact details: CSIRO Atmospheric Research
Private Bag No.1 Aspendale Victoria 3195 Australia
Ph: (+61 3) 9239 4400; fax: (+61 3) 9239 4444
e-mail: chief@dar.csiro.au

CSIRO Atmospheric Research Technical Papers may be issued out of sequence.

# In-flight characteristics of the space count of NOAA AVHRR channels 1 and 2

R.M. Mitchell
CSIRO Atmospheric Research
Private Bag 1, Aspendale,
Vic 3195, Australia

**Abstract**

The determination of space count from NOAA/AVHRR is critically examined. Application of simple statistical procedures to determine mean and standard deviation leads to biased estimates since the digitization interval is large compared to the noise. An alternative procedure is to fit a Gaussian to the measured probability distribution. Using this method, a compilation of space counts from four AVHRR instruments is presented. The period covered is from August 1992 to August 1994 (NOAA 11), August 1992 to December 1994 (NOAA 12), August 1994 to December 1994 (NOAA 9), and January to September 1995 (NOAAA 14). The stability and noise level of the data show marked differences between the two channels and between the same channel on different satellites. In particular, channel 2 of NOAA 11 showed significant but continuous excursions over the last year of its life, while channel 1 of NOAA 12 displayed notable discontinuities. Deviations in these cases are in the range 0.3 to 0.5 count, significantly larger than the system noise ($\sim$0.2 count). These excursions are of significance for applications involving dark targets, such as the retrieval of aerosol optical depth and the detection of suspended sediment in the ocean, confirming the need to use real time space count data rather than the pre-flight intercept approach commonly used.

# 1 Introduction

The visible and near-infrared channels of the AVHRR instrument on NOAA series satellites are commonly referred to as being without in-flight calibration. This arises from the fact that there is no on-board radiance source or solar diffuser provided to determine changes in instrument responsivity over time. Hence, responsivity must be determined vicariously using terrestrial targets whose radiance can be measured or inferred. Various techniques have been developed to achieve this (eg, Abel *et al.* 1993, Rao and Chen 1995, Che and Price 1993, Mitchell *et al.* 1995).

Often overlooked in this work is the role of the zero radiance offset in defining the baseline of the AVHRR shortwave calibration. The main signal amplifiers in the AVHRR operate by amplifying the difference between the output of the detector-preamplifier and a reference signal, whose voltage is set using the 1.6 ms 'radiometer space sample' obtained on each revolution of the scan mirror (ITT 1982). During this period, the input reference

signal is set using a feedback circuit that clamps the amplifier's output to a predetermined level, nominally 250 mV, leading to a nominal digital output of 40 counts. The reference input signal is then held fixed for the remainder of the scan line, so that the instrument's response to the scene ideally is proportional to the difference between the scene radiance and the space reference radiance. This clamping procedure is adopted to ensure that the output of the main amplifier remains within the dynamic range of subsequent signal processing hardware, regardless of possible drifts in the detector or preamplifier.

The clamping level is set using a stable reference voltage, so it has been assumed that the space count does not vary over time. This assumption led to the calibration equations currently recommended by NOAA/NESDIS, where the space count is assumed invariant either implicitly in the linear regression based on pre-flight data (Lauritson *et al.* 1979 and updates to Appendix B), or explicitly as in the AVHRR Pathfinder calibration (Rao and Chen 1995). However, more recent work suggests that it may not be valid to assume an invariant value for the space count. In particular, Teillet and Holben (1994) sampled the in-flight space view data from several AVHRR instruments on a number of occasions, and provided coefficients to enable interpolation in time. However, their work was concentrated on changes in responsivity, and to date there has been no systematic investigation of in-flight space count characteristics.

This paper seeks to fill this gap by presenting a time series of space counts obtained directly from AVHRR data over the period August 1992 to September 1995. This has been achieved by analysing the space view data that are present in the HRPT data stream at the rate of ten samples per scan line. These samples are acquired during the space-look portion of the scan mirror rotation, following the 'radiometer space sample' discussed above.

Four NOAA satellites are included in the study: NOAA 9, NOAA 11, NOAA 12 and NOAA 14. Two of these, NOAA 11 and NOAA 12, are studied over an extended period (two or more years), while data for NOAA 9 and the more recently launched NOAA 14 are limited to a few months. The space count data are analysed using archived statistics obtained from full-resolution overpasses. Section 2 points out that digitization errors can arise if simple statistical methods are used to determine the space count. Section 3 describes the data set acquired and suggests an alternative means of determining space count characteristics based on fitting a Gaussian distribution to the measured histogram. Resulting time series of space counts are presented and discussed in section 4. Further discussion and recommendations arising from these results are presented in section 5.

# 2 Digitization effects in pre-flight calibration

Pre-flight calibration data from ITT Calibration and Alignment Handbooks form a natural baseline for the present study. The following discussion reviews some relevant aspects of the laboratory calibration procedure.

Pre-flight calibration of the AVHRR is performed by directing the entrance aperture of the instrument so that its scan traverses both the opening of an integrating sphere, and a simulated space target. The radiance of the sphere may be varied over the dynamic range of the instrument by changing the number of lamps illuminated, and its radiometric output is traceable to a NIST reference source (see Rao 1987 for further details). During a calibration run, the response of the AVHRR is determined on the basis of its output signal following analogue to digital conversion. In particular, for each illumination level of the integrating sphere, the digital output is sampled 3600 times, made up of 360 revolutions of the scan mirror at 10 samples per revolution. An identical statistical sample is accumulated for each sphere level during the period when the AVHRR views the space target. The mean count and standard deviation computed from these samples form the basis of the calibration. The pre-flight space count is simply the mean count recorded when no lamps in the integrating sphere are illuminated. The system noise is determined from the 'combined average' of two quantities: first, the standard deviation of the output signal averaged over all illumination levels; and second, the standard deviation of the space target signal averaged over all illumination levels. For historical reasons, the AVHRR Calibration and Alignment Handbooks always tabulate these quantities in units of millivolts, even though the primary measurements are in digital counts.

Unfortunately, this statistical approach entails digitization errors, that are significant at the sub-count level since the system noise is less than the digitization interval. Thus the mean and standard deviation computed on the basis of the distribution of digital counts contain small errors, which vary depending on the relationship of the analogue signal to the digitization grid. This follows since in the computation of simple statistical quantities, the input signal within a given digitization level is reduced to a single value, assumed to act through the centroid of the digitization level, even though the true location may be anywhere within $\pm 0.5$ count of the centroid. In general, the computed mean and standard deviation will reproduce the characteristics of the original analogue signal only if the probability distribution of the input signal is constant or varies linearly across the digitization level.

To quantify this effect, we assume that the space count signal prior to analogue to digital conversion conforms to a Gaussian distribution with mean $\overline{x}$ and standard deviation $\sigma$, so that the probability distribution may be written

$$P(x) = \frac{1}{\sigma\sqrt{2\pi}} \exp\left(-\frac{1}{2}\frac{(x-\overline{x})^2}{\sigma^2}\right) \tag{1}$$

with $x$ and $\sigma$ measured in counts. Following analogue to digital conversion, we suppose that the digitized signal is sampled repeatedly, so that statistically significant probabilities may be assigned to a number of digitization levels. Defining $\mathcal{P}_i$ to be the probability that the count $x$ lies in the range $x_i \pm \frac{1}{2}$, where $x_i$ denotes the centre of the $i^{\text{th}}$ digitization interval, then a change of independent variable to

$$y = \frac{1}{\sqrt{2}}\frac{x-\overline{x}}{\sigma} \tag{2}$$

allows $\mathcal{P}_i$ to be written

$$\begin{aligned}\mathcal{P}_i &= \frac{1}{\sqrt{\pi}} \int_{y_i-\frac{1}{2}\Delta y}^{y_i+\frac{1}{2}\Delta y} dy\ \exp(-y^2) \\ &= \frac{1}{2}\left(\mathrm{erf}(y_i + \frac{1}{2}\Delta y) - \mathrm{erf}(y_i - \frac{1}{2}\Delta y)\right) \end{aligned} \tag{3}$$

where $\mathrm{erf}(y)$ is the error function,

$$\mathrm{erf}(x) = \frac{2}{\sqrt{\pi}} \int_0^x dx\ \exp(-x^2),$$

$$y_i = \frac{1}{\sqrt{2}} \frac{x_i - \overline{x}}{\sigma},$$

and

$$\Delta y = \frac{1}{\sigma\sqrt{2}}.$$

To investigate digitization errors, simulated probability distributions were generated by fixing $\sigma$, and then introducing an offset between the symmetry axes of the probability distribution and the digitization grid used to sample it. Specifically, the mean $\overline{x}$ was offset by an amount $x_{\mathrm{off}}$ from the centre of the most populous or mode digitization interval $x_{\mathrm{mode}}$, i.e.,

$$x_{\mathrm{off}} = \overline{x} - x_{\mathrm{mode}}. \tag{4}$$

Simple means and standard deviations were computed from

$$\begin{aligned}\overline{x}_s &= \sum_i x_i \mathcal{P}_i \\ \sigma_s^2 &= \sum_i (x_i - \overline{x}_s)^2 \mathcal{P}_i.\end{aligned}$$

Digitization errors in the mean and standard deviation were then computed as

$$\begin{aligned}\delta\overline{x} &= \overline{x}_s - \overline{x} \\ \delta\sigma &= \sigma_s - \sigma.\end{aligned}$$

Values of $\delta\overline{x}$ and $\delta\sigma$ are shown plotted in Figure 1 as functions of $x_{\mathrm{off}}$ for $\sigma = 0.2$, representative of typical AVHRR noise levels (see below). The diagram shows that $\delta\overline{x}$ can reach $\pm 0.15$ count while $\delta\sigma$ can reach 0.3, an error of 150%.

The variation of these errors with signal noise level is shown in Figure 2 for fixed values of $x_{\mathrm{off}}$. The effect of digitization error becomes negligible for $\sigma \geq 0.5$, at which point however $\delta\sigma$ may be as high as 0.1.

These findings have significance both for in-flight determination of space count, and for pre-flight calibration practices. The effect of digitization errors on the space count is

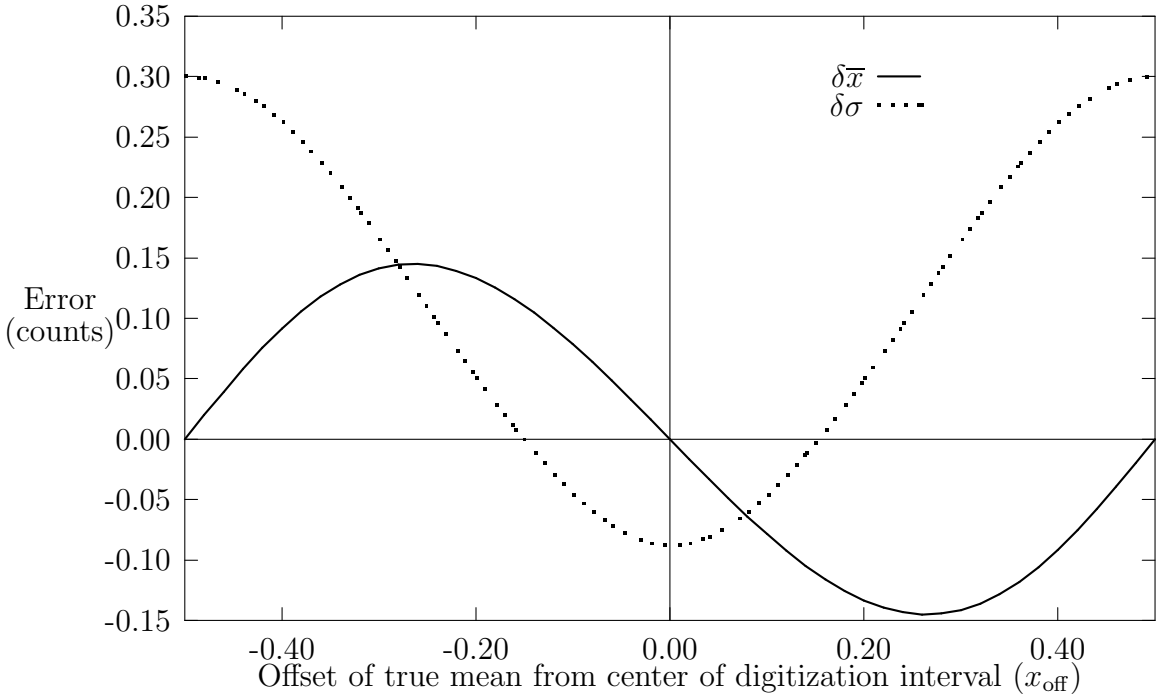


Figure 1: Digitization errors in calculated mean and standard deviation as a function of $x_{\rm off}$, the offset between the true mean and the centre of the digitization interval. The true standard deviation is 0.20.

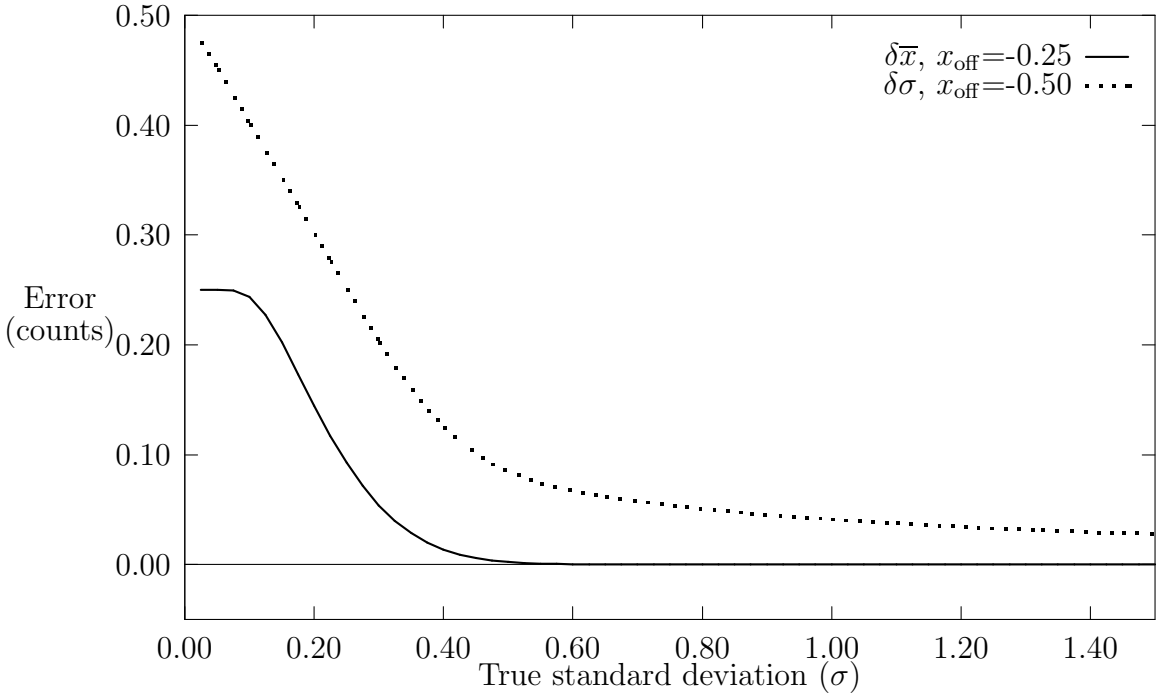


Figure 2: Digitization errors in calculated mean and standard deviation as a function of the true standard deviation, for fixed values of $x_{\rm off}$, the offset between the true mean and the centre of the digitization interval. The error in calculated mean is shown for $x_{\rm off}$ =-0.25, while the error in standard deviation is shown for $x_{\rm off}$ =-0.50.

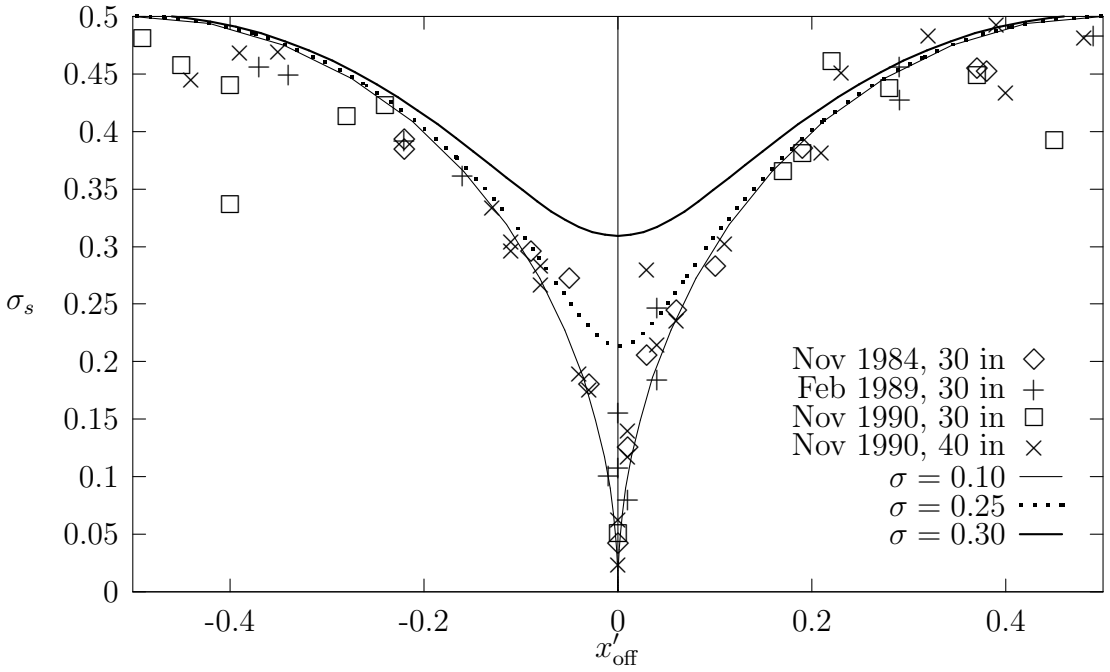


Figure 3: Comparison of standard deviation tabulated for SN205, the AVHRR on NOAA 12, with theoretical results based on the assumption that the noise on the analogue signal is Gaussian. The data are for four different calibrations of SN205. The two calibrations conducted in November 1990 are distinguished by the use of different integrating spheres, of sizes 30 inch and 40 inch respectively. The theoretical functions were computed for true standard deviations of 0.1, 0.25 and 0.3 counts.

modest (typically $\leq 0.15$ count), but still important in the context of monitoring long-term drifts and comparing pre-flight and in-flight space data.

Regarding pre-flight calibration procedures, noise figures determined on the basis of a single statistical sample of digitized AVHRR output contain an error of order 100% depending on the chance alignment of the analogue signal with the digitization grid. The practice of basing the noise figure on the average of many such determinations will ameliorate this, but the effect will remain since half the standard deviations on which the 'combined average' is based come from the space view, which will contain the same bias error in all samples.

Figure 3 confirms the validity of this picture by comparing the theoretical dependence of calculated standard deviation with data obtained from four separate calibrations of SN205, the AVHRR on NOAA 12 (ITT 1991). Note that the abscissa in Figure 3 differs from that in Figure 1 since the count value tabulated by ITT includes the digitization error discussed above, so that

$$x'_{\rm off} = \overline{x}_s - x_{\rm mode}.$$

The theoretical functions provide a good representation of the data for an analogue noise

| Satellite | Acquisition period | Number of passes |
|---|---|---|
| NOAA 9 | August 1994–December 1994 | 449 |
| NOAA 11 | August 1992–September 1994 | 2283 |
| NOAA 12 | August 1992–December 1994 | 2273 |
| NOAA 14 | January 1995–February 1995 | 404 |

Table 1: Summary of the space count data sets.

level in the range 0.1 to 0.25 count. Values tabulated in ITT (1991) range from 0.28–0.39 counts for the mean over all signal levels, while inclusion of the space view data reduces the 'combined average' to 0.22–0.28, a fortuitous result of the fact that the space count is near the centre of its digitization level. Clearly, alternative methods should be used to make the reported pre-flight standard deviation more representative of the noise on the analogue signal (see below).

# 3 Data set and analysis

The data set was assembled using the AVHRR reception facility at CSIRO Atmospheric Research. The extraction of space counts from the HRPT was automated so that data were gathered and archived for every pass successfully received. A summary of the data set is shown in Table 1.

Only passes containing 5,000 or more space count samples were included in the data set. Since a typical overpass consists of ∼5,000 lines, the number of samples per overpass is usually about 50,000 per channel. Before archiving, the data were processed to determine the mode count. Then five count bins were allocated above and below the mode count, and the data were assigned to one of the eleven resulting bins. Counts outside this range were flagged as outliers and discarded. A sample archived data record is shown in Table 2.

In-flight space count data were analysed by fitting Gaussian distributions to these archived histograms. First, the number of counts in each of the eleven bins was normalised by dividing by the total number of counts in the pass, yielding a set of probabilities $\mathcal{P}_i$. Next, a Gaussian distribution was fitted to the binned probabilities by numerical solution of the optimization problem

$$\underset{\overline{x},\,\sigma}{\text{minimize}} \sum_{i=1}^{M} \left( \text{erf}(y_i + \frac{1}{2}\Delta y) - \text{erf}(y_i - \frac{1}{2}\Delta y) - 2\mathcal{P}_i \right)^2, \tag{5}$$

which follows from equation (3). The number of bins used in the optimization, $M$, was set by requiring the probability to exceed an empirically determined threshold in the range 0.002–0.005. For a total sample of 50,000 this sets the minimum bin population in the range 100–250. In most cases this restricts $M$ to two or three, although it sometimes reached nine.

| Count | Channel 1 | Channel 2 |
|---|---|---|
| <35 | 8 | 7 |
| 35 | 1 | 1 |
| 36 | 0 | 5 |
| 37 | 0 | 2 |
| 38 | 2 | 3 |
| 39 | 3194 | 16967 |
| 40 | 46708 | 32894 |
| 41 | 9 | 3 |
| 42 | 1 | 0 |
| 43 | 0 | 0 |
| 44 | 0 | 0 |
| 45 | 0 | 0 |
| >45 | 60 | 98 |

Table 2: Sample data record: NOAA 11 orbit 19976, August 8, 1992.

Sample histograms for the four AVHRRs are plotted in figures 4–7, together with fitted Gaussian distributions. In most cases, more than 98% of the counts are divided between two digitization levels. The notable exception is channel 2 of NOAA 12, where $> 99.99\%$ of the counts are found in one digitization level. Indeed, many histograms show not a single count outside this digitization level. The Gaussian fitting procedure could not be applied in this case since at least two functions (i.e. $M \geq 2$) are required to ensure a unique solution to equation (5).

During the first two months' operation of NOAA 14, the AVHRR exhibited different space count characteristics depending on whether the overpass took place on the sunlit or dark side of the earth. Figure 7 shows sample histograms for both cases during this period.

| Satellite | AVHRR | Channel | Space count | | Noise | |
|---|---|---|---|---|---|---|
| | | | Pre-flight | In-flight | Pre-flight | In-flight |
| NOAA 9 | SN 202 | 1 | 39.20 | 37.99 | 0.34 | 0.30 |
| | | 2 | 40.00 | 39.59 | 0.32 | 0.19 |
| NOAA 11 | SN 203 | 1 | 40.96 | 40.27 | 0.30 | 0.22 |
| | | 2 | 40.30 | 40.10 | 0.38 | 0.27 |
| NOAA 12 | SN 205 | 1 | 41.00 | 40.91 | 0.28 | 0.21 |
| | | 2 | 40.41 | — | 0.38 | — |
| NOAA 14 | SN 204 | 1 | 41.31 | 40.94 | 0.34 | 0.17 |
| | | 2 | 41.96 | 40.98 | 0.26 | 0.20 |

Table 3: Comparison of pre-flight space count and noise determined from simple statistics, with those determined in-flight using Gaussian fitting.

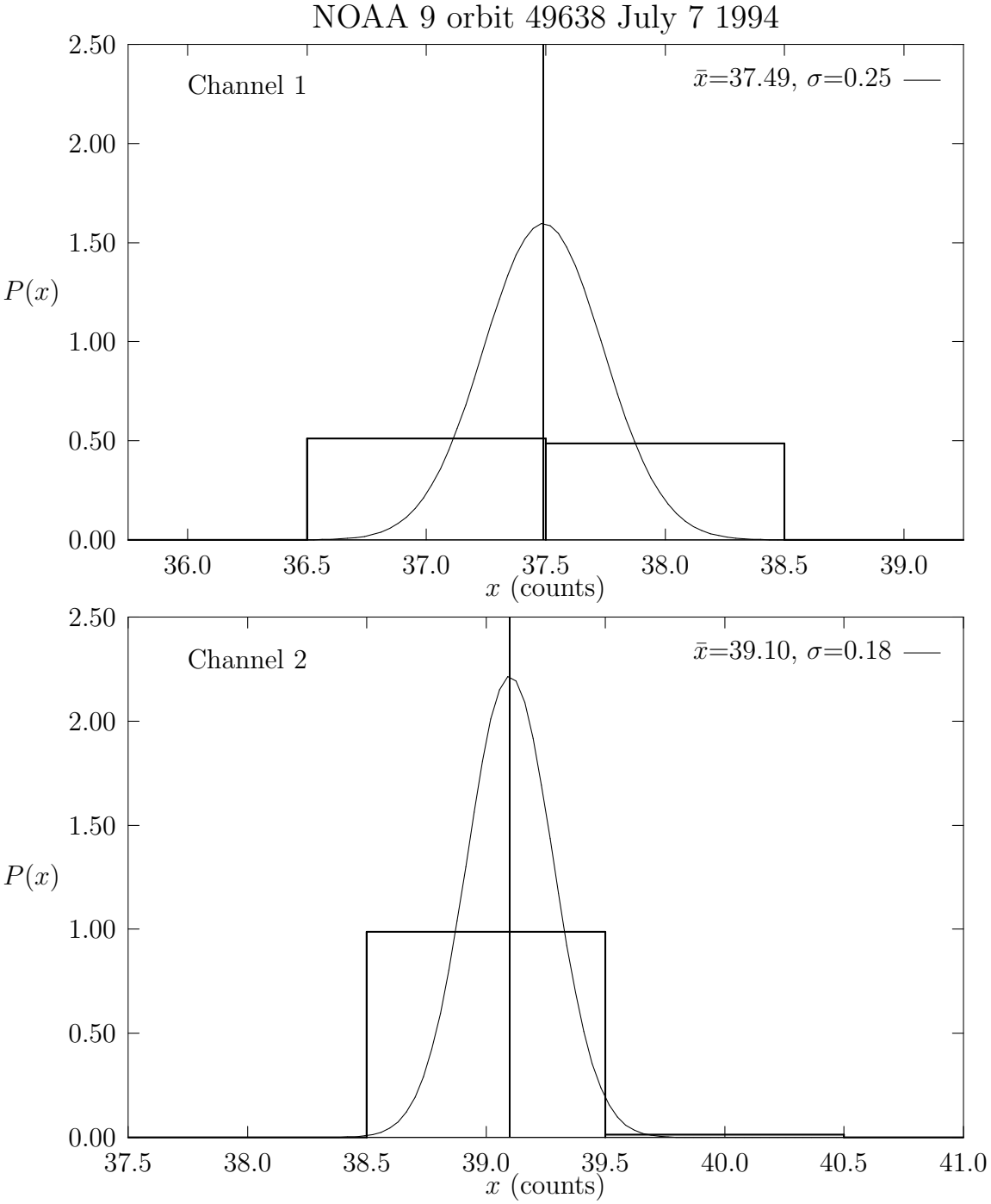


Figure 4: Space count statistics for NOAA 9 AVHRR obtained on July 7, 1994. The heavy lines indicate the histogram of space count normalized by the total number of observations, while the light line shows the fitted Gaussian distribution. Upper panel: channel 1; lower panel: channel 2.

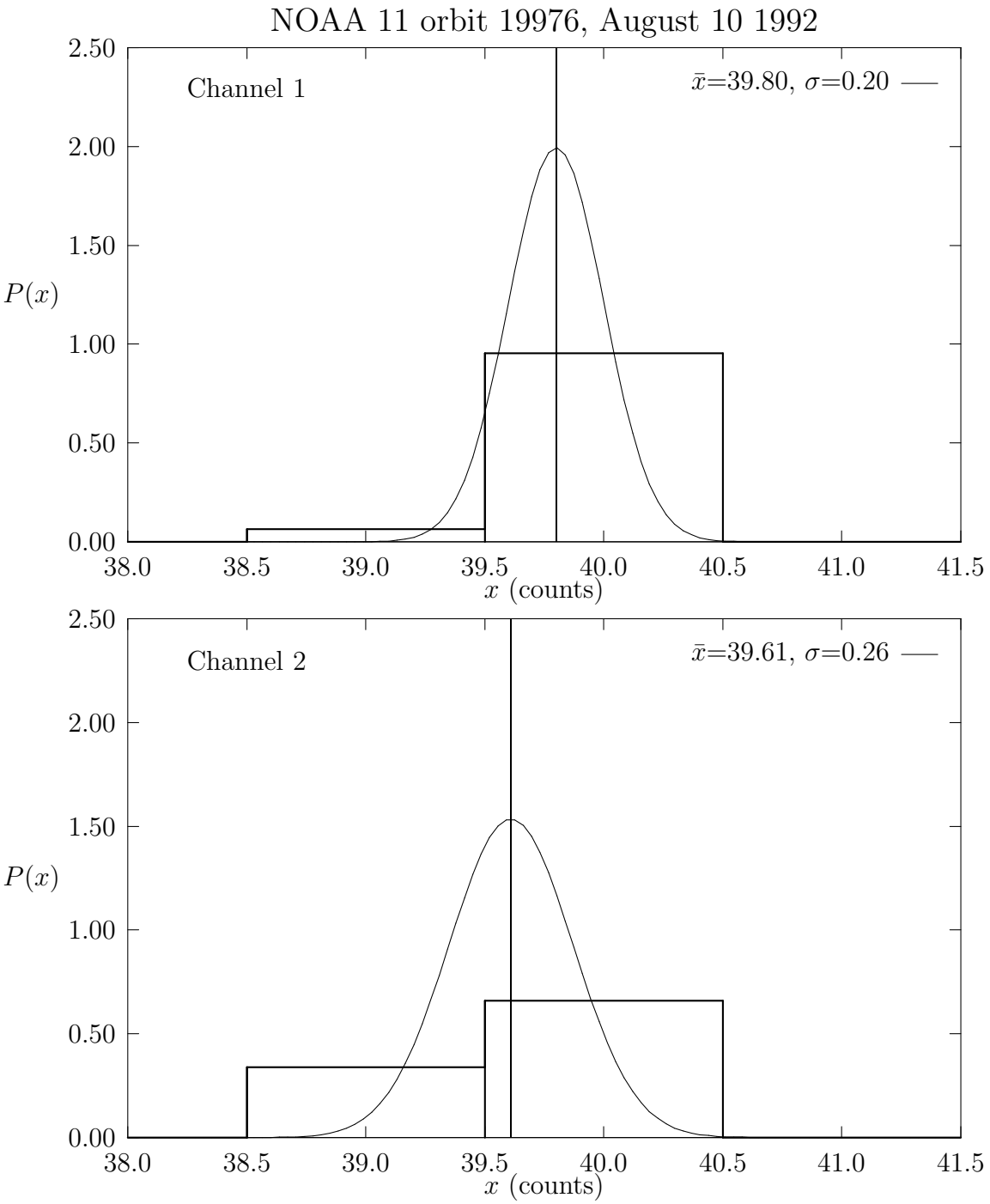


Figure 5: Space count statistics for NOAA 11 AVHRR obtained on August 10, 1992. The heavy lines indicate the histogram of space count normalized by the total number of observations, while the light line shows the fitted Gaussian distribution. Upper panel: channel 1; lower panel: channel 2.

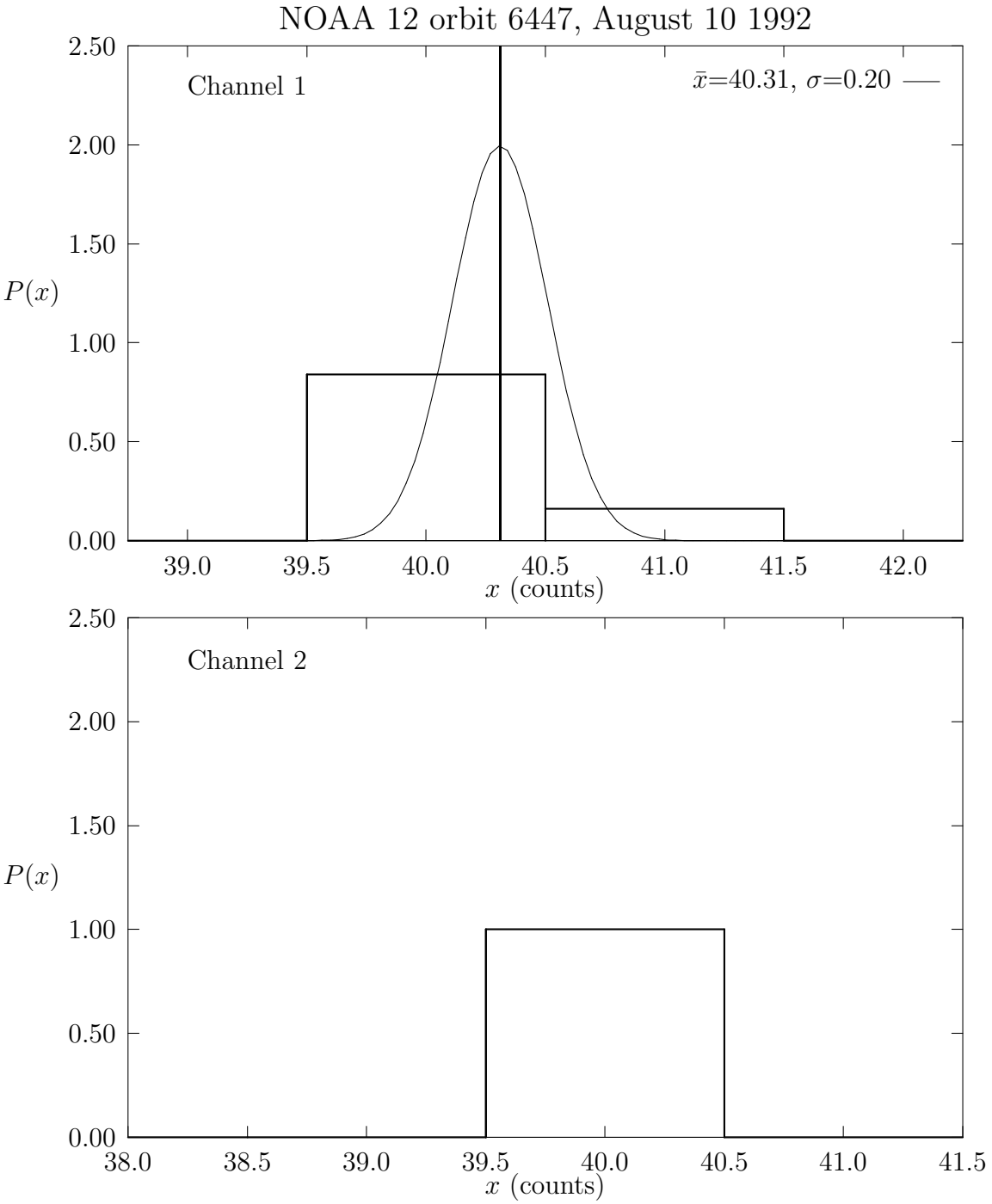


Figure 6: Space count statistics for NOAA 12 AVHRR obtained on August 10, 1992. The heavy lines indicate the histogram of space count normalized by the total number of observations, while the light line shows the fitted Gaussian distribution. Upper panel: channel 1; lower panel: channel 2. In channel 2 there were insufficient counts outside the central digitization level to enable the fitting proceedure to be applied.

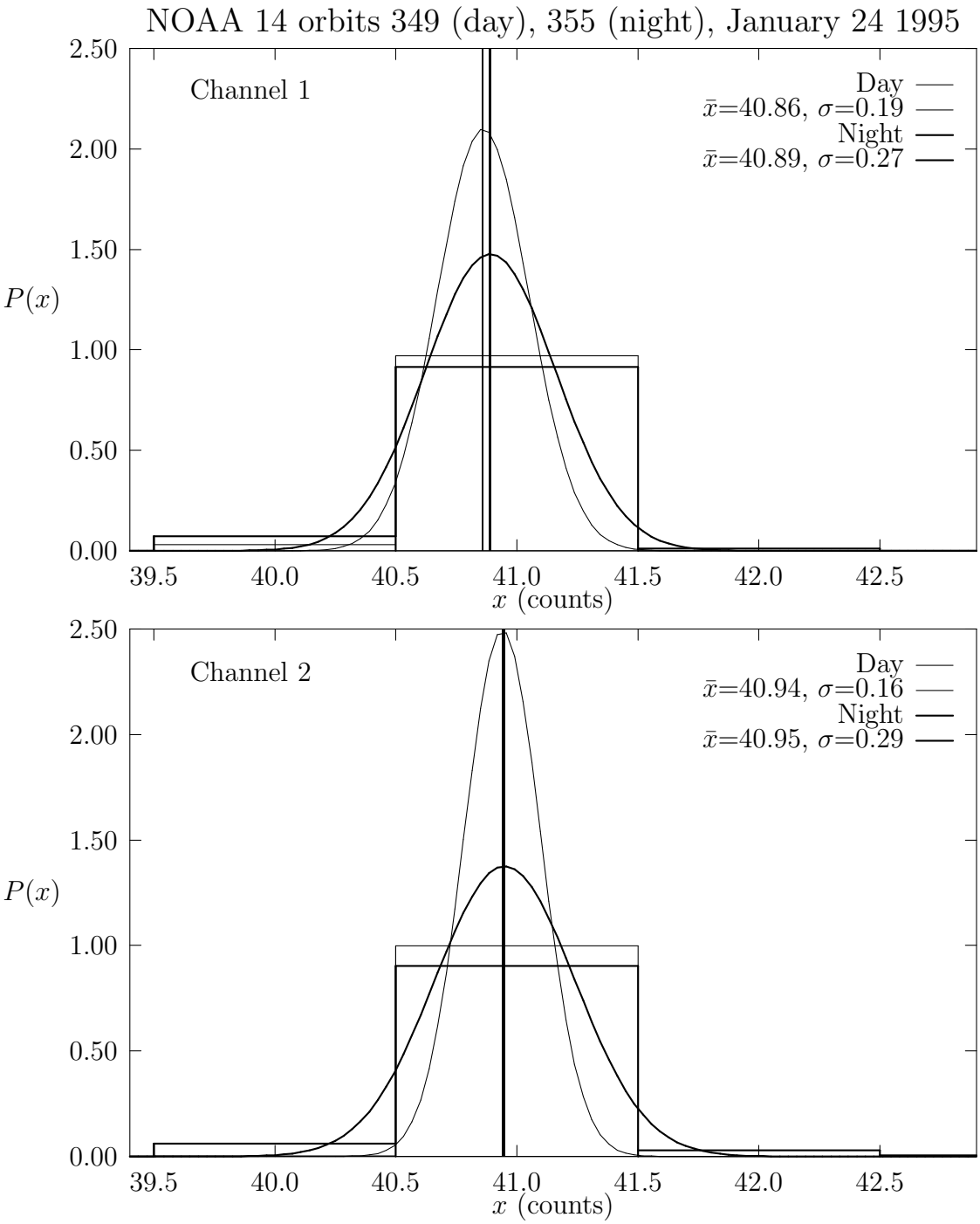


Figure 7: Space count statistics for NOAA 14 AVHRR obtained on January 24, 1995. The light lines show the histogram and fitted Gaussian distribution for the daytime overpass, while the heavy lines are for the nighttime pass about ten hours later. Upper panel: channel 1; lower panel: channel 2.

# 4 Results

A summary of pre-flight and in-flight space count characteristics is shown in Table 3. The pre-flight space count and noise were taken from ITT Calibration and Alignment Handbooks (ITT 1992, 1994a). The pre-flight noise values are based on the 'combined average' approach used by ITT, as discussed above in section 2. The in-flight values shown in Table 3 were obtained by averaging the results of the Gaussian fitting procedure over the respective time series.

The time series themselves are shown in figures 8, 9, 10 and 11 for NOAA 9, 11, 12 and 14 respectively. Mean space count $\overline{x}$ and standard deviation $\sigma$ were determined using the Gaussian fitting method discussed above. Error bars of amplitude $\pm 1\sigma$ are plotted for every twentieth data point to avoid undue clutter, except for NOAA 14 where error bars are shown for every fourth point (channel 1) and all points (channel 2). Where available, piecewise linear fits of Teillet and Holben (1994) are also shown.

## 4.1 NOAA 9

The AVHRR on this satellite has been in continuous operation since its launch on December 12 1984. Routine acquisition of NOAA 9 imagery at Aspendale ceased during the lifetime of NOAA 11, but resumed with the failure of the AVHRR on the latter satellite in September 1994. Hence the temporal baseline is comparatively short. In channel 1 the extrapolation based on the recommendation of Teillet and Holben is $\sim$0.3 count below the measured value, while in channel 2 the agreement is within 0.1 count. Channel 1 is noticeably more noisy than channel 2, with in-flight noise estimates of 0.30 count in channel 1 and 0.19 count in channel 2. Both values fall below the pre-flight determinations of 0.34 and 0.32 count respectively, an expected result of the digitization errors present in the pre-flight calculations.

## 4.2 NOAA 11

Time series for this instrument are shown in figure 9(a) and 9(b) for channels 1 and 2 respectively. The predictions of Teillet and Holben in channel 1 lie above the measurements by 0.1 count during 1992, but during the latter part of 1993 the predictions and measurements coalesce. This agreement continues until the instrument's demise. Channel 2 shows similarly stable behaviour up until mid August 1993 when an upward trend began. The trend culminated in a maximum deviation of 0.3 count from the Teillet and Holben prediction by the end of 1993. During 1994 there is further mildly erratic behaviour, ending in a steady decline over the six weeks prior to instrument failure.

Noise characteristics are the reverse of NOAA 9, in that channel 2 is more noisy than

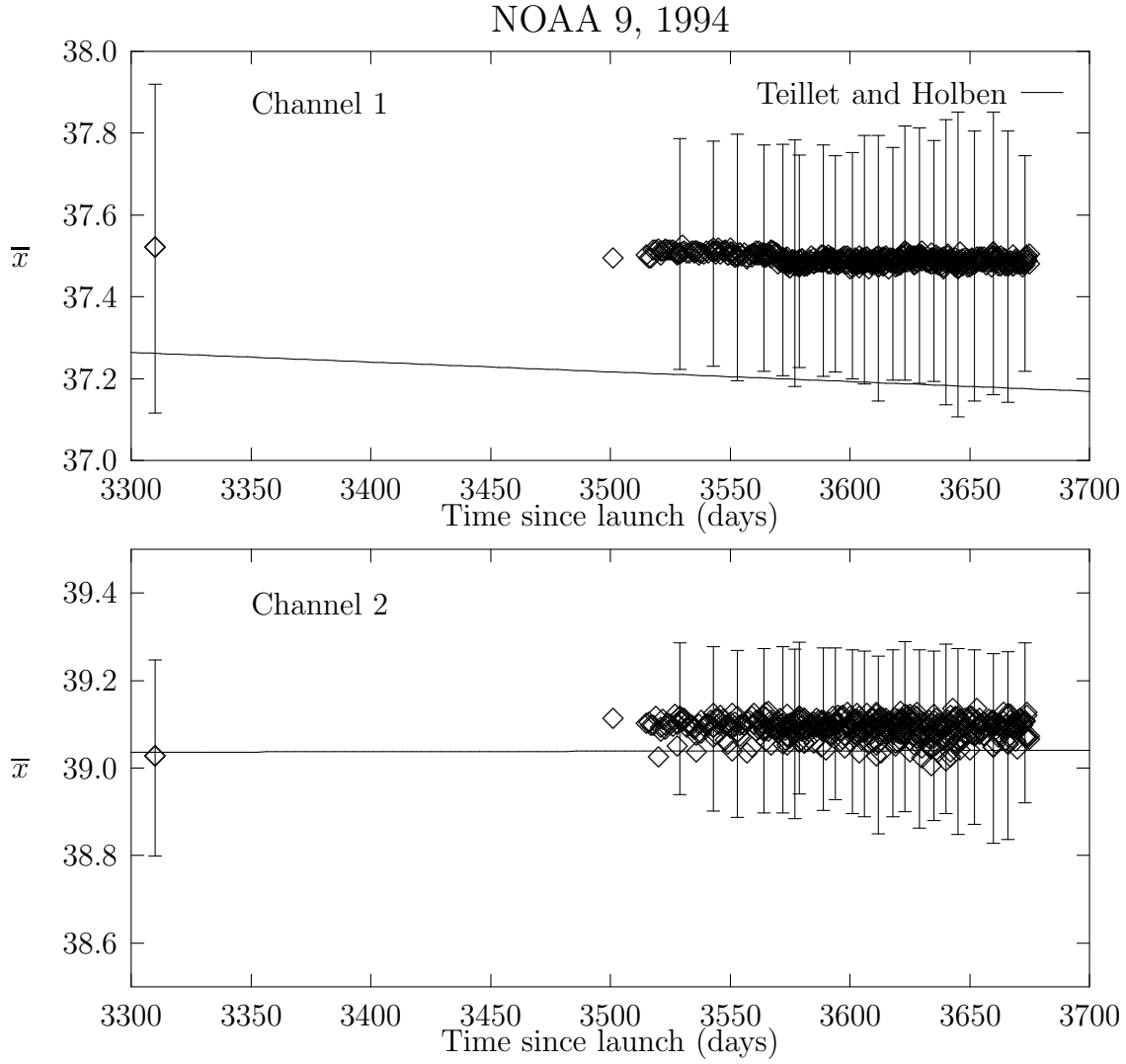


Figure 8: Time series of NOAA 9 AVHRR space count. Error bars are $\pm 1\sigma$. The continuous line shows the piecewise linear function recommended by Teillet and Holben. Upper panel: channel 1; lower panel: channel 2.

channel 1 both pre-flight and in-flight. Pre-flight noise values of 0.30 and 0.38 count may be compared with in-flight values of 0.22 and 0.27 respectively. Once again, this discrepancy is consistent with the digitization error present in the pre-flight values.

## 4.3 NOAA 12

Channel 1 of NOAA 12, the time series of which is shown in figure 10, demonstrates bizarre characteristics. During the period between mid 1992 and mid 1993 the space count was relatively stable, although there is some evidence for split-level behaviour, with signal levels separated by ∼0.07 count. However, around June 8 1993 the space count increased discontinuously from 40.3 to 40.6 count. Over the next ten weeks the space count rose a further 0.2. After reaching a maximum of near 40.9 counts, it fell back to its previous level on September 2. This behaviour was repeated in mid 1994. This time the period of elevated space count lasted about 80 days, between May 9 1994 and August 7 1994. During both periods of elevation, there is some evidence for an increase in pass-to-pass variation of mean space count. Teillet and Holben recommended the adoption of a space count of 40.0 for this channel. The observed values are consistently higher than this, by up to 0.9 counts during the first elevated period. The observed noise level on this channel was near 0.21 count, marginally lower than the pre-flight determination of 0.28.

As discussed above, the fitting technique could not be applied to channel 2 of NOAA 12 because the noise is insufficient relative to the digitization interval. This is unexpected, since the pre-flight noise measured on channel 2 was 0.38 count, significantly greater than that in channel 1 (0.28 count). This arises because the pre-flight space count of 40.41 ($x_{\text{off}}$ = -0.41) leads to a large digitization error in the 'space standard deviation' of 0.48 count. By contrast, the standard deviation averaged over all sphere levels was only 0.27 count.

## 4.4 NOAA 14

The time series for this satellite is shown in figure 11. In channel 1 there is evidence for a systematic difference between daytime and nighttime overpasses of ∼0.1 count prior to day 60. This is illustrated more clearly in figure 12, which shows retrieved standard deviation $\sigma$ plotted against mean count $\overline{x}$ over this period. Both $\overline{x}$ and $\sigma$ are consistently higher for the nighttime overpasses. This difference disappears after day 60, accompanied by an increase in mean space count from 40.9 to 41.0. This effect points to a change in performance or operating environment of the voltage reference source used to set the space count. The diurnal difference soon after launch may be associated with temperature variations, but the reason for the change after day 60 is puzzling.

The space count for channel 2 is shown in the lower panel of figure 11. Of a total of 404 samples, only 93 had sufficient counts outside the central digitization level to qualify for analysis, even with the probability threshold reduced to 0.002.

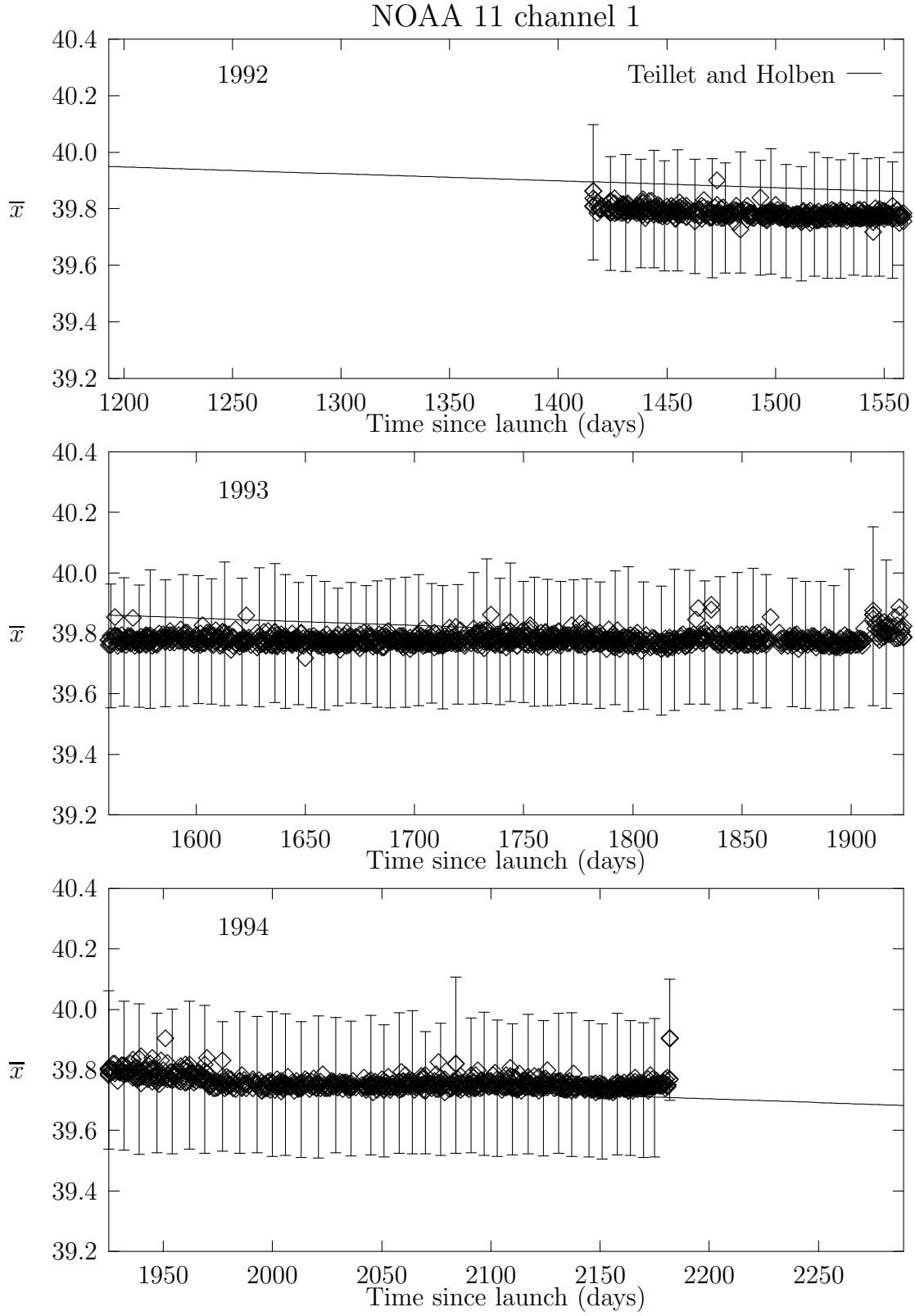


Figure 9(a): Time series of NOAA 11 AVHRR space count in channel 1. Errror bars are $\pm 1\sigma$. The continuous line shows the piecewise linear function recommended by Teillet and Holben. Upper panel: 1992; middle panel: 1993; lower panel: 1994.

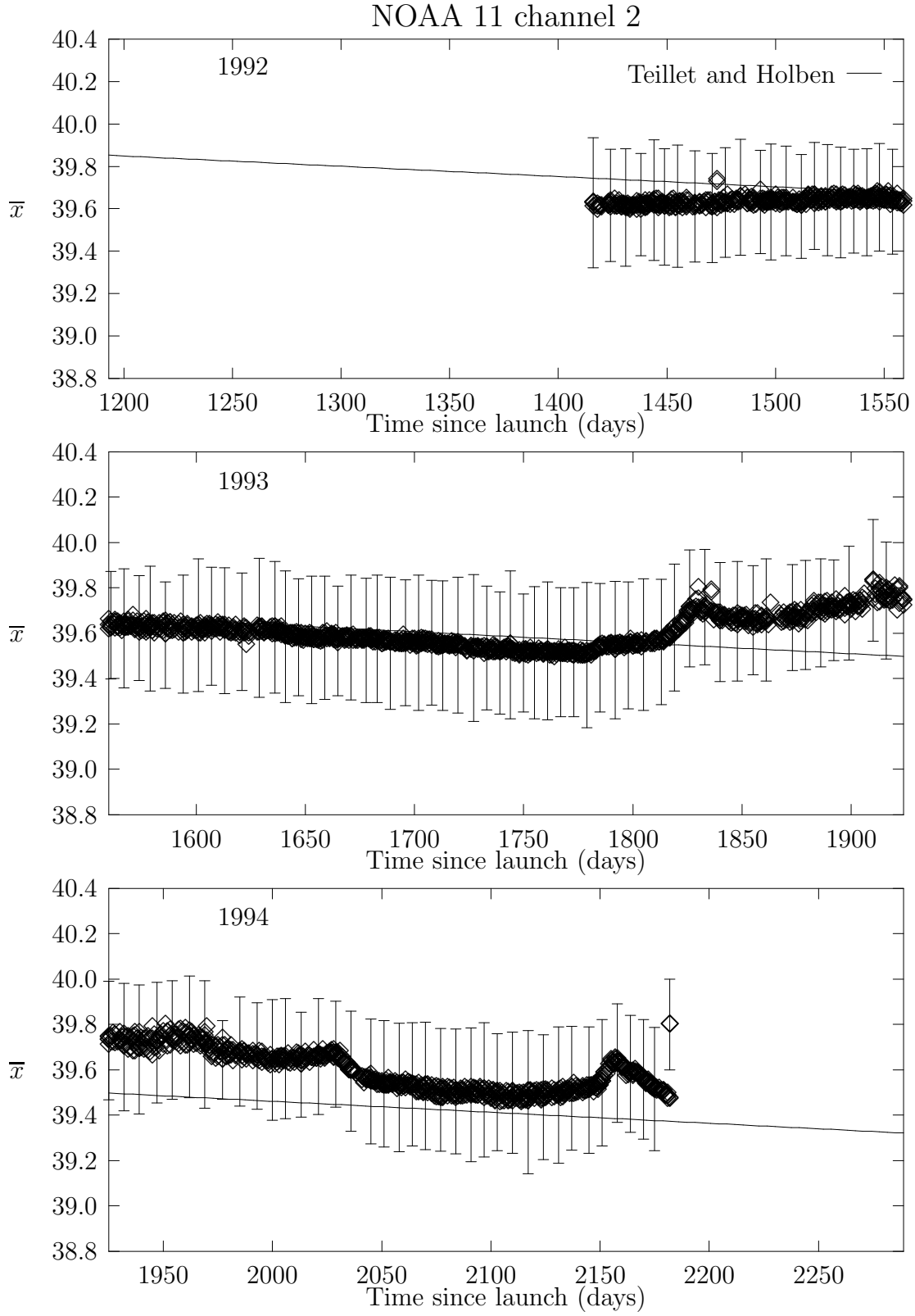


Figure 9(b): Time series of NOAA 11 AVHRR space count in channel 2. Errror bars are $\pm 1\sigma$. The continuous line shows the piecewise linear function recommended by Teillet and Holben. Upper panel: 1992; middle panel: 1993; lower panel: 1994.

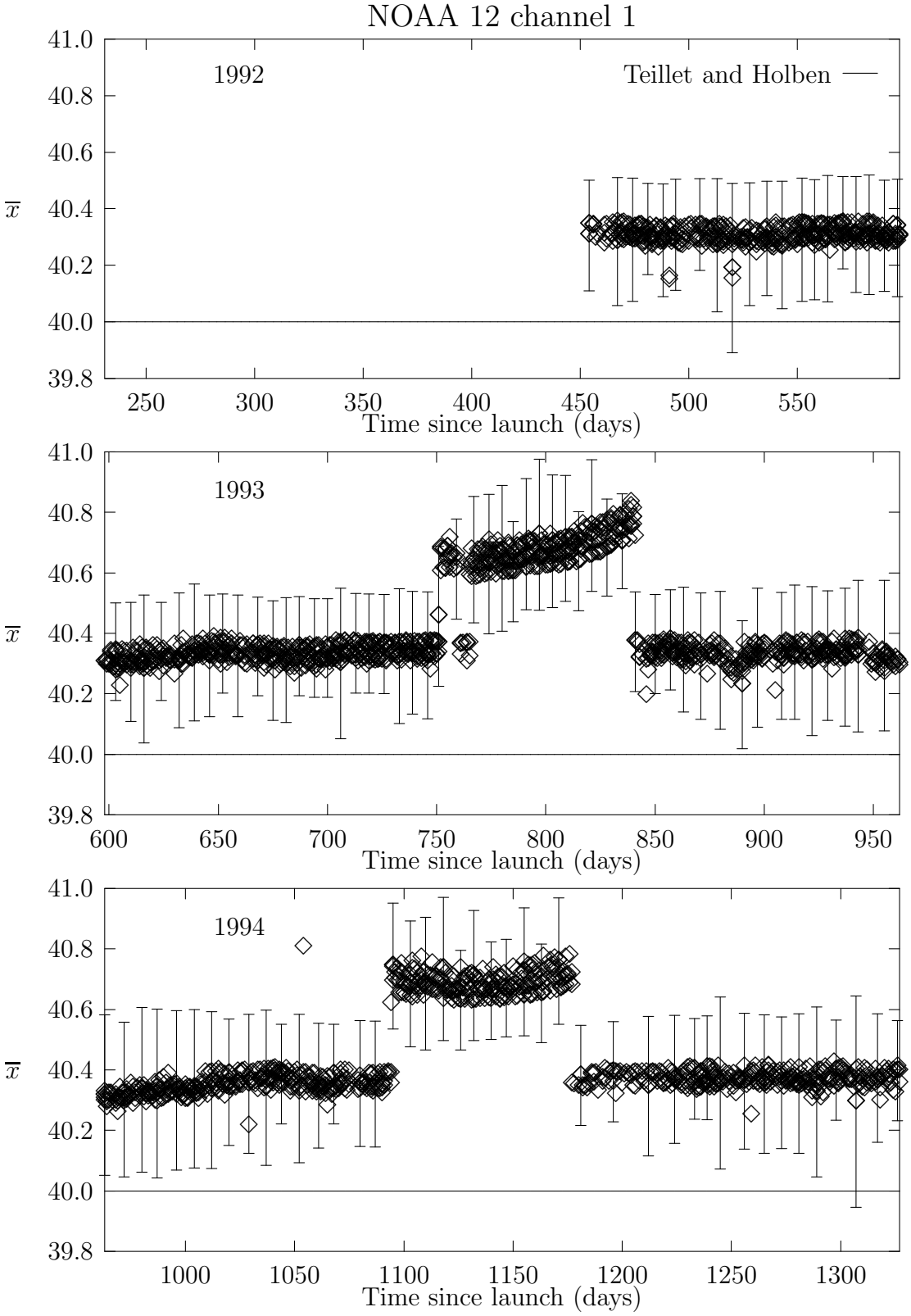


Figure 10: Time series of NOAA 12 AVHRR space count in channel 1. Errror bars are $\pm 1\sigma$. The continuous line shows the piecewise linear function recommended by Teillet and Holben. Upper panel: 1992; middle panel: 1993; lower panel: 1994.

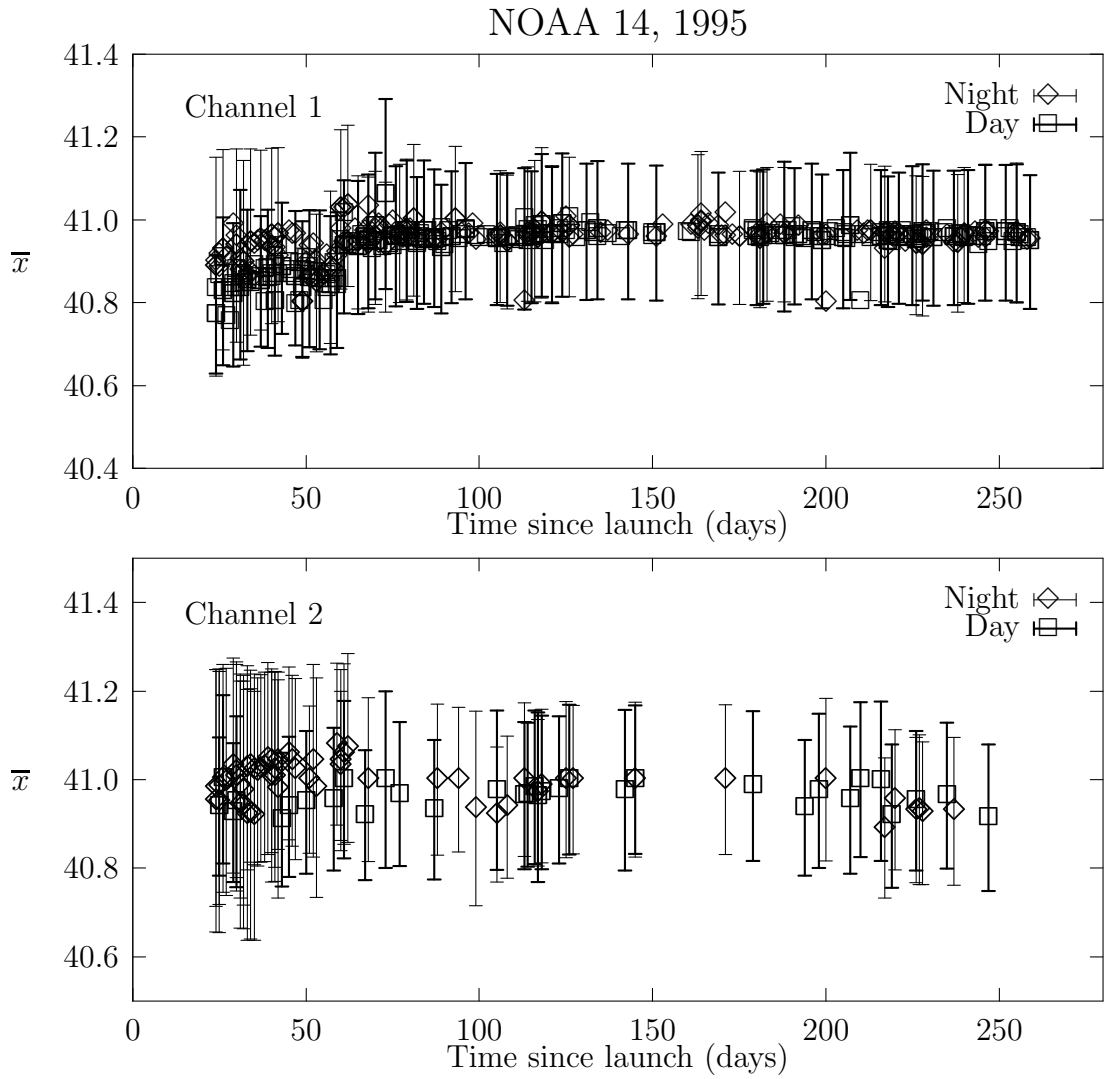


Figure 11: Time series of NOAA 14 AVHRR space count. Upper panel: channel 1; lower panel: channel 2.

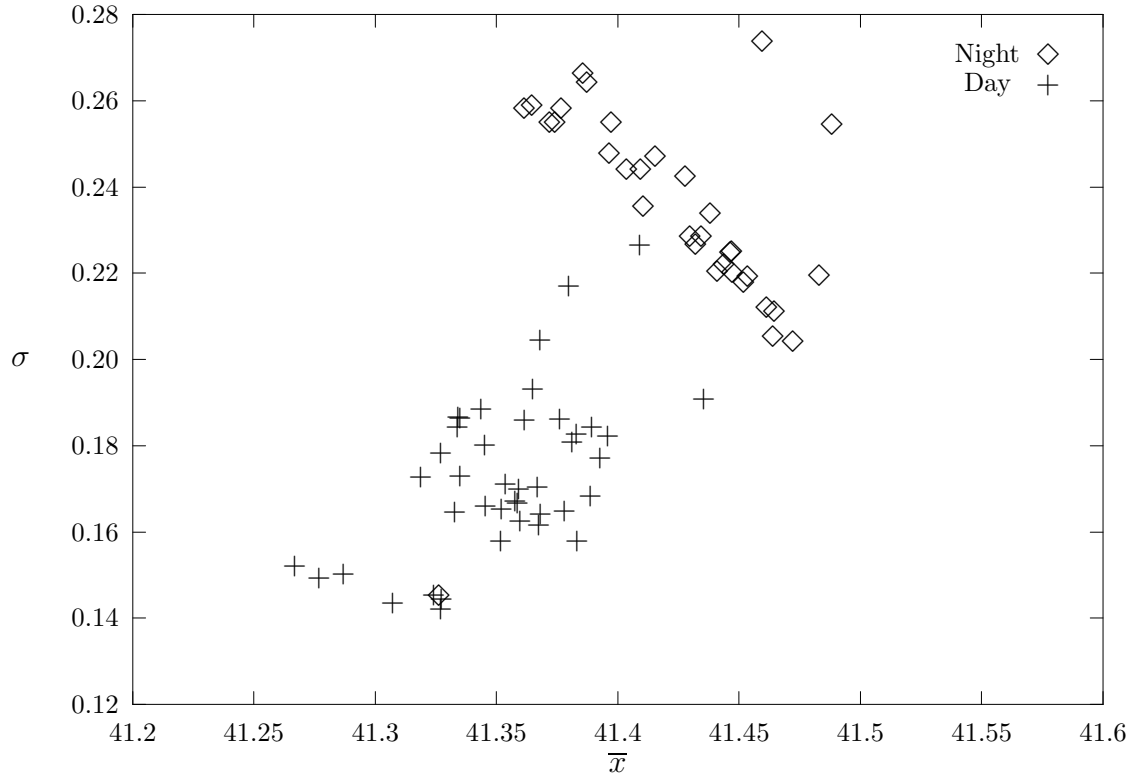


Figure 12: Scatter plot of recovered standard deviation $\sigma$ versus mean space count $\overline{x}$ during the first two months' operation of the NOAA 14 AVHRR, channel 1.

## 4.5 Long-term drift

Table 4 summarizes long-term drift in space count for NOAA 9, 11 and 12. Drifts were computed as

$$d = \frac{C_0(0) - C_0(t^*)}{t^*}$$

| Satellite | Channel | Period $t^*$ (yr) | Drift (count yr$^{-1}$) |
|---|---|---|---|
| NOAA 9 | 1 | 10.0 | 0.120 |
| | 2 | 10.0 | 0.040 |
| NOAA 11 | 1 | 5.89 | 0.122 |
| | 2 | 4.80 | 0.058 |
| NOAA 12 | 1 | 3.43 | 0.035 |

Table 4: Long-term drift performance

where $C_0(0)$ is the pre-flight space count listed in table 3 and $C_0(t^*)$ is the in-flight space count obtained from figures 8–10. The time $t^*$ was chosen to exclude periods of anomalous behaviour seen above in NOAA 11 channel 2 and NOAA 12 channel 1. NOAA 9 and NOAA 11 show consistent results, and comparison of drifts in the two channels suggests that channel 1 drifts more rapidly than channel 2 by a factor of between two and three.

# 5 Discussion

## 5.1 Impact on small-signal applications

The relative error in radiance $I$ due to an error in space count $\delta C_0$ is

$$\frac{\delta I}{I} = \frac{\delta C_0}{C - C_0}, \tag{6}$$

where $\delta C_0$ is the difference between a published space count value and that determined in-flight. As seen above, $\delta C_0$ values are generally of the order of one count or less, so this error is only significant for small-signal applications involving dark targets. Examples of such applications are retrieval of aerosol over the ocean (Rao *et al.* 1989), and the remote sensing of aquatic sediments (Stumpf and Pennock 1989).

By way of example, counts observed over the ocean away from sunglint for clean maritime conditions are typically in the range $20 < C - C_0 < 50$ (channel 1) and $10 < C - C_0 < 30$ (channel 2). For NOAA 12 channel 1, $\delta C_0 \sim 0.8$ count during the periods of elevation seen in figure 10, so that $\delta I/I$ is in the range 1.6% to 4.0%. For NOAA 11 channel 2, the deviation of $\delta C_0 \sim 0.3$ count near the end of 1993 leads to $\delta I/I$ in the range 1% to 3%. The upper values of these ranges are of the same order as the uncertainty present in vicarious determinations of the in-flight gain, which is in the range 3 to 5% for individual methods (e.g. Abel *et al.* 1993) and typically 5% when an ensemble of results is considered (Mitchell *et al.* 1995). Hence for these small-signal applications, it is important to use space count values determined in-flight, rather than published pre-flight values (see also Abel 1990).

## 5.2 Recommended minimum noise level

As noted above, channel 2 of NOAA 12 has insufficient noise to enable a determination of space count at the sub-count level. This situation is undesirable, since the actual space signal may lie anywhere within the digitization level, leading to a possible bias error of up to one count. Hence it is recommended that a minimum noise level be introduced as part of the design specification. This noise level should be high enough to ensure that a significant number of counts are distributed across two or more digitization intervals in a sample size of ∼50,000. Experience with the present method suggests that a noise value of about 0.3 count provides the best tradeoff between the requirement for minimal

NE$\Delta\rho$ whilst retaining the feasibility of in-flight space count determination to sub-count resolution. This is consistent with matching the analogue noise level to the rms digitization error of $\frac{1}{\sqrt{12}} = 0.29$ count inherent in any analogue to digital conversion.

This situation appears unlikely to be realized in channels 1 and 2 of AVHRR/3 to fly on NOAA KLM, where rms noise levels for a space view are equivalent to 0.068 and 0.025 count respectively (ITT 1994b). If these noise levels are maintained in flight, all space samples will appear in a single digitization level, preventing the determination of space count to sub-count resolution. However, the response function for these channels has been changed relative to AVHRR/2 so that the reflectance range 0–25% occupies half the dynamic range (500 counts), effectively doubling the radiometric resolution (1 count $\sim$ 0.05% reflectance). Hence the digitization error is correspondingly less severe. In the new channel 3a (1.6$\mu$m) the ITT (1994b) calculations suggest a space view noise of 0.56 count so that sub-count resolution of the space count should be possible. The response function for this channel allocates the reflectance range 0–12.5% to the first 500 counts, so that 1 count $\sim$ 0.025% reflectance. In this case, accurate determination of space count will be important for proposed low radiance applications such as retrieval of aerosol optical depth over the oceans.

## 5.3 Revised determination of space count

As illustrated above, the current method used by ITT to determine pre-flight noise performance is subject to a systematic overestimate of order 100% due to digitization error. A smaller but significant error is also present in the determination of the space count itself when a simple average is used to calculate it. The present paper has suggested an improved method of calculating the space count properties in-flight by fitting a Gaussian to the recorded histogram. It is recommended that, where possible, present simple statistical procedures be abandoned in favour of a method such as this. The advantages of this change would include not only a more accurate characterization of pre-flight sensor performance, but would also lead to improved radiometric accuracy for low radiance applications. To ensure uniformity among the user community, it would be helpful if the task of monitoring space count status could be undertaken by a central agency such as NOAA, augmenting existing calibration activities.

## Acknowledgements

The author wishes to thank Drs M.P. Weinreb, C.R.N. Rao, P.J. Turner and A. Ignatov for helpful discussions, and Mr Clive Elsum for assistance with data acquisition and processing. The cover image was provided courtesy of Mr R.P. Galvin, ITT Aerospace/Communications. This work was undertaken while the author held a UCAR visiting fellowship at NOAA/NESDIS Office of Research Applications, Satellite Research Laboratory, on leave from CSIRO Atmospheric Research.

## 5.4 References

Abel, P. (1990): Prelaunch calibration of the NOAA-11 AVHRR visible and near IR channels, *Remote Sensing of Environment*, **31**, 227–229.

Abel, P., Guenther, B., Galimore, R.N. and Cooper, J.W. (1993): Calibration results for NOAA-11 AVHRR channels 1 and 2 from congruent path aircraft observations, *J. Atmos. Oceanic Technol.*, **10**, 493–508.

Che, N. and Price, J.C. (1993): Improved method for calibrating the visible and near-infrared channels of the National Oceanic and Atmospheric Administration Advanced Very High Resolution Radiometer, *Applied Optics*, **32**, 7471–7478.

ITT (1982): Advanced Very High Resolution Radiometer, Technical Description, NAS5-26771, *ITT Aerospace/Optical Division, Fort Wayne, Indiana*.

ITT (1991): Final report for the AVHRR and HIRS instrument support, AVHRR/2 Calibration CH 1 and CH 2 (S/N 205 & S/N 206) 30" and 40" integrating spheres, Contract NAS5-30887, Task order 7B, *ITT Aerospace/Communications Division, Fort Wayne, Indiana*.

ITT (1992): Advanced Very High Resolution Radiometer, Calibration Data, NAS5-29114, *ITT Aerospace/Communications Division, Fort Wayne, Indiana*.

ITT (1994a): Advanced Very High Resolution Radiometer/2, Alignment and Calibration Handbook, SN 204, *ITT Aerospace/Communications Division, Fort Wayne, Indiana*.

ITT (1994b): Technical description for the Advanced Very High Resolution Radiometer AVHRR/3, NAS5-30384, *ITT Aerospace/Communications Division, Fort Wayne, Indiana*.

Lauritson, L., Nelson, G.J. and Porto, F.W. (1979): Data extraction and calibration of TIROS-N/NOAA radiometers, NOAA Tecnical Memorandum NESS 107.

Mitchell, R.M., O'Brien, D.M., and Forgan, B.W. (1995): Calibration of the NOAA AVHRR shortwave channels: II. Application to NOAA 11 during early 1991, *Remote Sensing of Environment, in press*.

Rao, C.R.N. (1987): Pre-launch calibration of channels 1 and 2 of the Advanced Very High Resolution Radiometer, NOAA Technical Report NESDIS 36.

Rao, C.R.N. and Chen, J. (1995): Inter-satellite calibration linkages for the visible and near-infrared channels of the Advanced Very High Resolution Radiometer on NOAA-7, -9, and -11 spacecraft, *Int. J. Remote Sensing*, **16**, 1931–1942.

Rao, C.R.N., Stowe, L.L. and McClain, E.P. (1989): Remote sensing of aerosols over the oceans using AVHRR data: Theory, practice and applications, *Int. J. Remote Sensing*, **10, 4–5**, 743–749.

Stumpf, R.P. and Pennock, J.R. (1989): Calibration of a general optical equation for remote sensing of suspended sediments in a moderately turbid estuary, *J. Geophys. Research*, **94, C10**, 14363–14371.

Teillet, P.M. and Holben, B.N. (1994): Towards operational radiometric calibration of NOAA-AVHRR imagery in the visible and near-infrared channels, *Canadian J. Remote Sensing*, **20(1)**, 1–10.